Advanced Powder Technology 28 (2017) 1399–1410

Contents lists available at ScienceDirect

Advanced Powder Technology

journal homepage: www.elsevier.com/locate/apt

Original Research Paper

Synthesis of hierarchical nanoporous HY zeolites from activated kaolin, a central composite design optimization study

Peter Adeniyi Alaba [a,*], Yahaya Muhammad Sani [b], Isah Yakub Mohammed [c], Yousif Abdalla Abakr [d], Wan Mohd Ashri Wan Daud [a]

[a] Department of Chemical Engineering, University of Malaya, 50603 Kuala Lumpur, Malaysia
[b] Department of Chemical Engineering, Ahmadu Bello University, 870001, Nigeria
[c] Department of Chemical Engineering, Abubakar Tafawa Balewa University, P.M.B. 0248, Bauchi, Nigeria
[d] Department of Mechanical, Materials and Manufacturing Engineering, The University of Nottingham Malaysia campus, 43500 Jalan Broga Selangor, Malaysia

ARTICLE INFO

Article history:
Received 20 April 2016
Received in revised form 19 December 2016
Accepted 11 March 2017
Available online 24 March 2017

Keywords:
HY zeolite
Hierarchical nonporous
Hierarchy factor
Relative crystallinity
Optimization
Tolerance interval

ABSTRACT

In this article, we investigated the optimum formulation towards synthesis of hierarchical nanoporous HY zeolites from acid activate kaolin. A central composite design (CCD) helped to examine the influence of aging (X_1), crystallization (X_2) and NaOH solution to kaolin ratio (X_3) on crystallinity (*C*%), specific surface area (SSA) and hierarchical factor (HF). From the analysis of variance (ANOVA), we deduced that all the process variables show statistical significance towards obtaining high *C*% and SSA while only X_3 is statistically significant for optimal HF. The effectiveness of models was further evaluated using margin of error and tolerance interval. The Optimum formulation for this hierarchical nanoporous HY zeolite was 43.60, 64.23 and 6.97 for X_1, X_2, and X_3, respectively. The developed models show that X_3 is the most statistically significant variable because it has the highest coefficient and the lowest *p*-value in the entire model. These results give instrumental insight into the synthesis of hierarchical nonporous HY zeolite.
© 2017 The Society of Powder Technology Japan. Published by Elsevier B.V. and The Society of Powder Technology Japan. All rights reserved.

1. Introduction

Y zeolites have gained vast popularity within the research community and commercially due to their uniform pore size, high specific surface area and thermal stability [1–3]. Rational design of this Fajausite materials requires tailored pore architecture as well as controlled location, strength, and nature of acid sites [4]. Despite the established methods for tuning the strength and nature of acid sites, controlling the location of active sites and pore architecture [4,5].

The utilization of Y zeolites is limited in processes that involve bulky molecules because they have relatively low pore size [6]. Such processes include organic waste treatment, heavy crude oil, and bio-oil upgrading because of the mass transfer limitation they pose to bulky chemical reaction. These highlight the rational for great effort dedicated to the synthesis of novel bimodal structured molecular sieves. These materials gained the term "hierarchical porous" because they synergistically combine the outstanding properties of mesoporous and microporous zeolites [7–9]. Hierarchical nanoporous materials exhibit high thermal and hydrothermal stability and possess unique pore channel with bimodal pore system (micro- and mesopores) [10–12]. Connecting microporous channels to mesoporous ones in a highly ordered form results in the microporous channels residing in the matrix causing shorter diffusion path for the reactant molecules [12–14].

Many variables influence formation of these faujasitic materials [15,16]. This informs the need to employ multivariate experimental design to scrutinize the statistically significant independent variables [1]. In this case, response surface methodology (RSM) is a viable optimization tool. The methodology employs central composite design (CCD) as one of the design tools for model fitting through least square method [17]. To investigate the suitability of the proposed model equation, analysis of variance (ANOVA) is a vital tool [17]. ANOVA provides diagnostic checking test for the model with Fisher's statistical test (*F*-test). Response surface plots help to provide the optimal response location and surfaces study. RSM also offers a robust evaluation of operation results and efficiency [17]. The literature is rife with several work done on Y zeolite synthesis [1,18,19], but few actually conducted optimization studies. Karami and Rohani [1] conducted optimization study for the synthesis of Y zeolite using soluble silicate and aluminum sulfate as silica and alumina source respectively in a two-level

* Corresponding author. Fax: +60 3796 75319.
E-mail addresses: adeniyipee@live.com (P.A. Alaba), ymsani@abu.edu.ng (Y.M. Sani), ashri@um.edu.my (W.M.A. Wan Dau).

http://dx.doi.org/10.1016/j.apt.2017.03.008
0921-8831/© 2017 The Society of Powder Technology Japan. Published by Elsevier B.V. and The Society of Powder Technology Japan. All rights reserved.

factorial design. However, the zeolite precursors are expensive. Chandrasekhar and Pramada [19] showed the prospect of producing Y zeolite from kaolin as a cheap source for both silica and alumina but the process variables are not systematically optimized.

In this work, an optimization study was conducted for the synthesis of hierarchical nanoporous HY zeolite from kaolin in a two-level full factorial design using CCD. The mathematical models were developed in terms of aging, crystallization and NaOH solution to kaolin ratio (NaS). This is to provide a quantitative evaluation of hierarchical factor (HF), crystallinity and specific surface area (SSA). The experimental design is made up of 20 run with the center point repeated 6 times. This is to ensure accurate measurement and satisfactory reproducibility towards producing pure hierarchical nanoporous HY zeolites.

2. Experimental

2.1. Materials

The kaolin (Si/Al = 1.06) used for this investigation is from R&M Chemicals Sdn. Bhd., Malaysia. The study used the reagents without further purification. R&M Chemicals Sdn. Bhd., Malaysia also supplied the NaOH and H_2SO_4 (95–98% pure).

2.2. Methods

The synthesis HY zeolites precursor was by thermal activation at 850 °C for 2 h and subsequent activation with 6 M H_2SO_4 at 90 °C for 2 h to produce amorphous aluminosilicate. The precursor was added to an aqueous NaOH solution (14%) at different NaOH/Solid ratio (ml/g). The solution was aged at room temperature for 4.4–43.6 h and subsequently crystallized at 100 °C for 8.8–87.2 h. This was followed by washing and filtering with distilled water using vacuum pump until pH of 4.1–13.9. Further, drying took place at 110 °C overnight and subsequently soaked in a solution saturated with NaCl to its equilibrium water content [19]. The essence of NaCl imbibement is to enhance the crystallinity and hydrothermal stability and maintain the initial porous structure [19,20]. However, excess salt collapse the mesopore wall of mesoporous materials [19,21]. Further, the samples were placed in a fume cupboard to remove excess water and dried. The samples were transformed into hydronium form in 0.2 M ammonium nitrate solution for 24 h. The filtering and drying of the resulting solution took place at 110 °C overnight and then calcination followed at 550 °C for 2 h. The resulting materials were designated HY36-72-6 for sample aged for 36 h, crystallized for 72 h using NaOH solution/solid ratio of 6.

2.3. Characterization

XRF analysis gives the silicon and aluminum composition of the synthesized HY zeolites. X-ray diffractometer (Philip Expert X-ray Diffractometer) helps to carry out the XRD analysis using nickel-filtered Cu Kα radiation ($\lambda = 1.544$ Å) ranging from 5.018 to 69.966° (2θ) with a step size of 0.026° for all the samples. The peak reflections at (511), (440), (533), and (642) helped to determine the relative crystallinity of the samples [22].

$$\textit{Relative Crystallinity}\ (\%) = \frac{\textit{Sum of sample characteristic peak area}}{\textit{Sum of the reference characteristic peak area}} \times 100 \quad (1)$$

The crystallite size of the aforementioned peaks was computed with the aid of PANalytical X'Pert HighScore software [23]. Further, we compared the crystallinity of the samples with that of conventional Y zeolite to obtain the values of relative crystallinity.

Perkin Elmer Spectrum RX FT-IR was used for the infrared spectroscopy (IR) to confirm Y zeolite fingerprint. Surface area and porosity analyzer (Micrometrics ASAP 2020) gave the nitrogen adsorption-desorption analysis using analysis bath temperature of 77.350 K.

The morphology of the synthesized HY zeolites was visualized by Scanning electron microscopy (SEM, FEI Quanta 400 FE-SEM) using 20 kV as the accelerating voltage. The HY zeolites samples were coated with gold, prior to the examination, to enhance the electrical conductivity.

2.4. Hierarchy factor

Hierarchy factor is a viable tool to categorize the degree of structural order of porous materials. This tells how less mesopore formation penalize the micropore formation of the synthesized zeolite sample [20,24–26].

Zheng et al. [26] proposed a model as a tool for classification of hierarchy mesoporous zeolites as derived from the conventional N_2 adsorption analysis. From the ratio of micropore volume to mesopore volume (V_{micro}/V_{meso}) and relative mesopore specific surface area (S_{meso}/S_{BET}) of the weighed sample, they defined hierarchy factor (HF) as follows:

$$\mathrm{HF} = \frac{V_{micro} * S_{meso}}{V_{meso} * S_{BET}} \quad (2)$$

where V_{micro} is the micropore volume; V_{meso} is the mesopore volume; S_{meso} is the specific surface area of the mesopore and S_{BET} is the BET surface area. The V_{micro}, V_{meso} and S_{meso} are obtained by using *t*-plot. The value of HF increases as V_{micro} and S_{meso} increases, whereas, it decreases with increase in V_{meso}.

2.5. Experimental design and data analysis

A two-level blocked full factorial design by CCD was conducted in which three process parameters was used. The parameters are aging, crystallization and NaOH solution to kaolin ratio were expressed as dimensionless (X_1, X_2, and X_3 respectively). The coded values are −1, 0, 1 for low, center and high level respectively. The process parameter levels selection was centered on the results of our earlier works [20].

Minitab® 16.2.2 was used for the regression and statistical analysis of the experimental data. The total number of runs is 20 which entails 8 cube point, 4 center points in a cube, 6 axial points, and 2 center points in axial. The distance between the center point and the axial point is α for low/high level while the remaining factors maintained their center values. That is, the axial points are situated at (0, 0, ±α), (0, ±α, 0) and (±α, 0, 0). Generally, α is a function of a number of factors, *k* and is given as $(2^k)^{0.25}$. Nevertheless, Minitab® 16.2.2 provides the user an option of choosing the value of α. The value of α used in this work is 1.633. The number of runs replicated at the center point served as materials for experimental error determination. The responses chosen for RSM study are crystallinity, SSA, and HF that were designated as Y_1, Y_2, and Y_3 respectively.

Table 1
Levels of HY zeolites Independent variables for the CCD.

Variable	Symbol	Coded variable levels		
		−1	0	1
Aging time (h)	X_1	12	24	36
Crystallization time (h)	X_2	24	48	72
NaOH to sample ratio (ml/g)	X_3	6	9	12

Table 2
CCD arrangement for the three process variable.

Run	Block	X_1	X_2	X_3
1	2	0	−1.633	0
2	2	0	0	−1.633
3	2	0	0	1.633
4	2	0	0	0
5	2	0	0	0
6	2	1.633	0	0
7	2	0	1.633	0
8	2	−1.633	0	0
9	1	1	−1	−1
10	1	1	1	1
11	1	0	0	0
12	1	0	0	0
13	1	−1	1	−1
14	1	−1	1	1
15	1	−1	−1	−1
16	1	1	−1	1
17	1	−1	−1	1
18	1	0	0	0
19	1	0	0	0
20	1	1	1	−1

Table 1 presents the CCD arrangement in a manner that permits modeling of the suitable empirical model (polynomial equation). The simplified form of this model is used to obtain the desired responses generally as:

$$Y = \beta_0 + \sum_{i=1}^{n}\beta_i X_i + \sum_{i=1}^{n}\beta_{ii}X_i^2 + \sum_{i=1}^{n}\sum_{j=i+1}^{n}\beta_{ij}X_iX_j + e \quad (3)$$

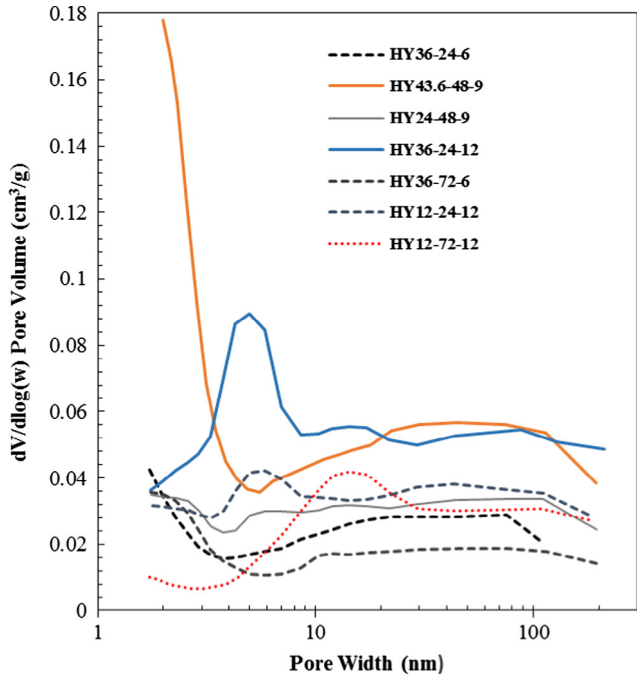

Fig. 2. Pore size distribution of some selected HY zeolites samples.

where X stands for the independent variables, β for the regression coefficients, e is the error and Y stand for modeled responses. β_0 is the offset term while $\beta_i X_i$ and $\beta_{ii}X_i^2$ are the linear effect and quadratic effect respectively, and $\beta_{ij}X_iX_j$ $(i \neq j)$ is the second order term.

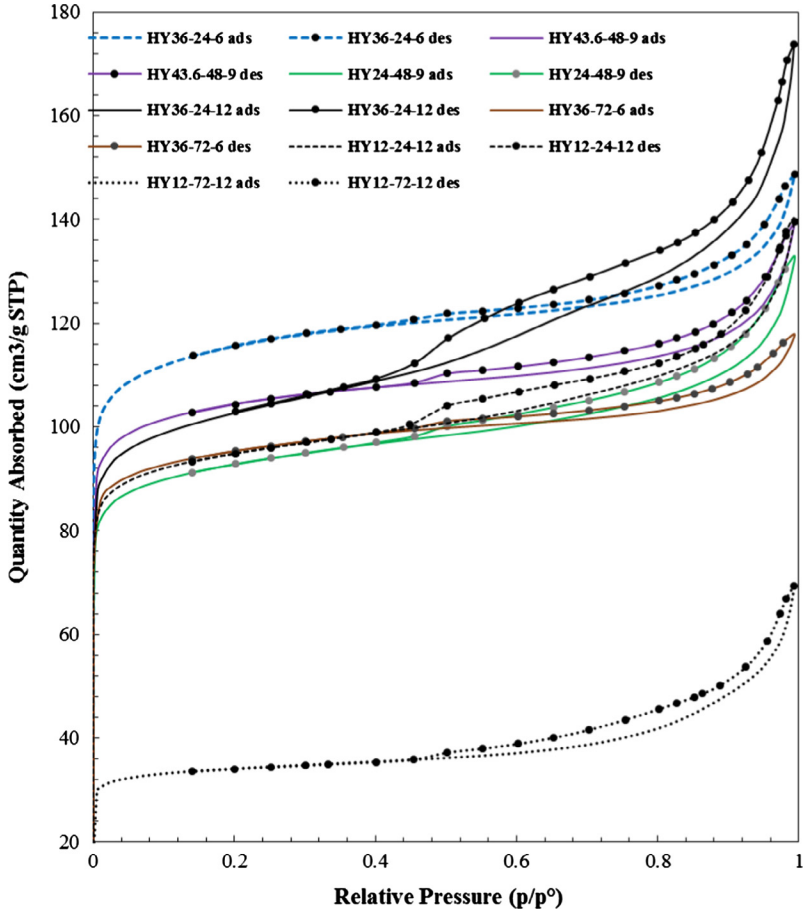

Fig. 1. Nitrogen adsorption/desorption isotherms of some selected HY zeolites samples.

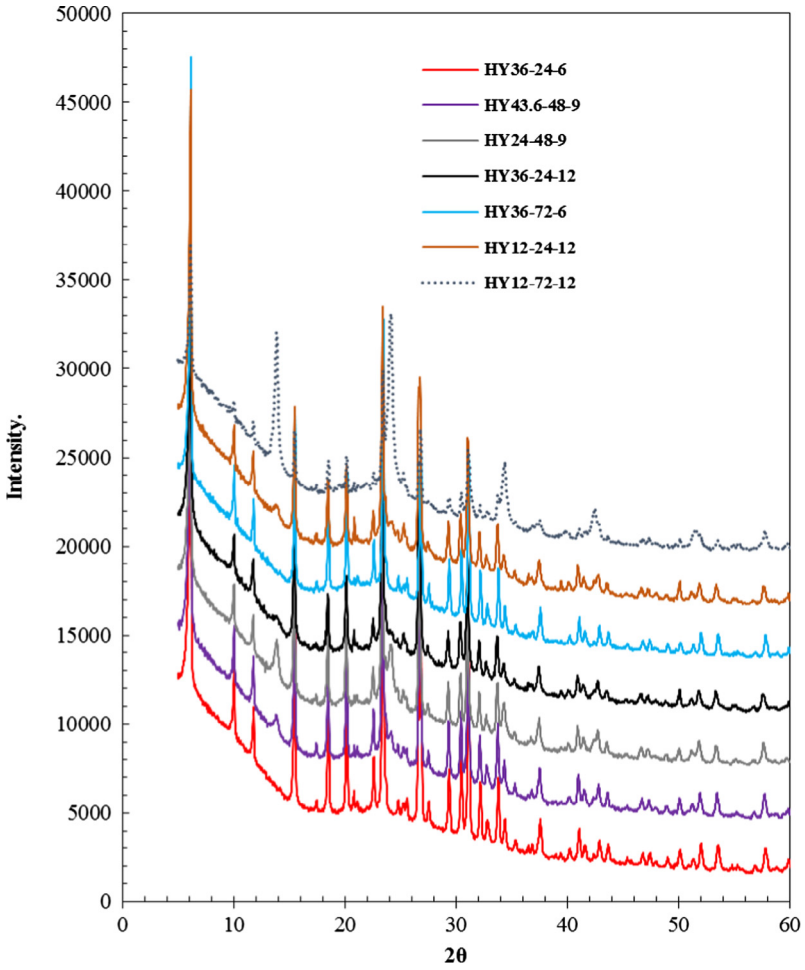

Fig. 3. Powder XRD pattern of some selected HY zeolites samples.

Table 3
Textural properties and composition of some selected HY zeolite samples.

Sample	Aging (h)	Crystallization (h)	NaOH/solid (ml/g)	Relative crystal (%)	BJH pore size (nm)	Si/Al	BET SSA (cm^2/g)	HF
HY12-24-12	12.00	24.00	12.00	74.93	8.98	1.59	366.90	0.20
HY24-48-9	24.00	48.00	9.00	76.62	8.61	1.52	359.06	0.23
HY36-24-6	36.00	24.00	6.00	106.86	8.03	1.88	443.78	0.30
HY36-24-12	36.00	24.00	12.00	63.79	8.46	1.53	394.84	0.18
HY36-72-6	36.00	72.00	6.00	87.29	6.81	1.83	367.34	0.32
HY36-24-6	43.60	48.00	9.00	85.64	7.15	1.67	406.14	0.23
HY12-72-12	12.00	72.00	12.00	31.32	14.66	1.43	133.24	0.11

The suitability of the proposed model was analyzed by ANOVA. ANOVA determines which of the operating parameters affect the responses significantly using *F*-test for diagnosis [17]. This determines the effects estimates of each parameter with respect to their magnitude and significance. Further, possible response models were obtained. The effect estimate is the anticipated improvement in the response as the process variables were varied from low to high. Terms with a *p*-value greater than 0.05 were discarded and regarded as 'residual error'. This was followed by a new ANOVA check. Note, the *p*-value is an index that measures the unreliability of a result [27].

Either *p*-value or *F*-value of the model and lack-of-fit is suitable for determination of model significance [28]. The ratio of the mean square (MS) of the process variable to the MS of the error terms gives the *F*-value while the *p*-value is obtained from *F*-distribution using the degree of freedom (DF) and the *F*-value of the process variable and that of the error term. DF is the amount of information provided by the data that can be used to estimate the values of unknown parameters. The value of DF depends on the sample size. Increase in sample size increases the value of DF ($DF = n - 1$).

The model shows significant lack-of-fit if the pure error is significantly lower than the residual. In this case, pure error rather than a residual error is suitable for determination of *F*-value [28]. Pure error is the residuals sum of squares estimated based on repeated runs only, which is used as a measure of experimental error.

The critical value of F for the model as well as the lack-of-fit are function of the degree of freedom of each term and that of their associated error terms [29]. If the *F*-value of the model is higher than its critical value and lack of fit *F*-value is less than its critical value, the regression model is acceptable. The model is also

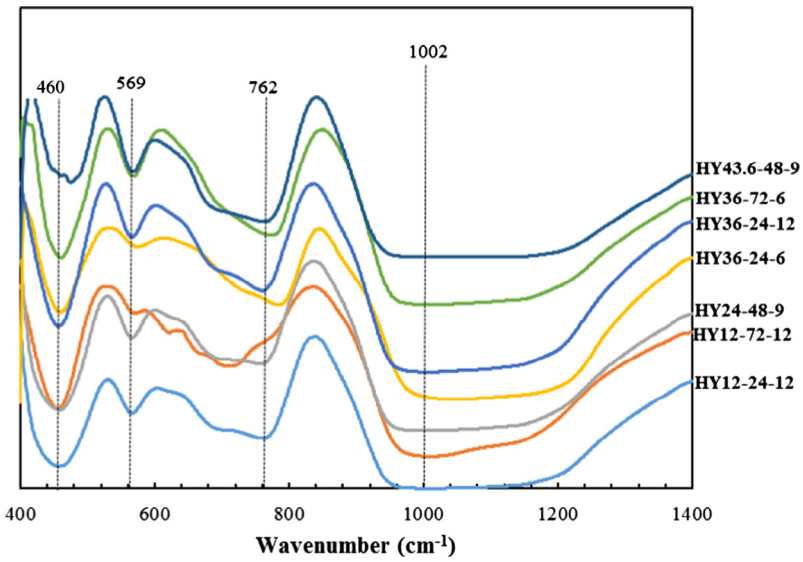

Fig. 4. FT-IR spectra of some selected HY zeolites samples.

acceptable if its *p*-value is less than 0.05 and its lack-of-fit is greater than 0.05. Else, the model is acceptable if not less than 95% of the data fit into the model (coefficient of multiple determination, $R^2 > 0.95$).

For further evaluation of the effectiveness of the models, the margin of error was estimated for the two-sided confident interval at 95% confidence level using standard deviation (normal). The margin of error expresses the random error that emanates from uncertainties or differences between the measured and the predicted value of a parameter [30]. This will enable appropriate interpretation of the result. Standard error solely depends on factors like the sample size, the amount of variation in the responses, and the data size for which the estimate was made [31]. For a two-sided alternative hypothesis, the margin of error is the distance from the estimated statistic to each confidence interval value. Wider confidence level gives a larger margin of error, and lesser reliability of the model [32]. Moreover, we assessed the quality of the synthesized samples by computing the tolerance interval. For a normal distribution, tolerance interval is a statistical procedure that gives the range in which, with some confidence level, a specific proportion of an experimented population falls. Tolerance interval has gained immense popularity among various statistical intervals, especially in manufacturing industries because it confidently satisfies the expectation of the manufacturers [33,34]. The intervals are wider than other statistical intervals such as confidence and prediction intervals. This enables it to provide limits of quantification and detection estimates [35].

3. Results and discussion

3.1. Hierarchical nanoporous HY zeolite characterization

The results of the textural properties, Si/Al molar ratio, and XRD peak areas are presented in Table 2, Figs. 1–3. The table shows samples textural parameters for some of the samples with respect to their operating conditions. It is evident from here that crystallinity, HF and SSA varies with aging time, crystallization time, NaOH/Solid. The relative crystallinity of HY36-24-6 is greater than 100% probably because the reference Y zeolite composes of a little amorphous part making the crystallinity of the synthesized samples higher than that of the reference sample. The increase in crystallization time also improves the textural properties of the samples but severe crystallization proved detrimental. Moreover, increase in NaOH/Solid from 6 to 9 ml/g leads to decrease in SSA, HF, Si/Al ratio and crystallinity of the sample.

The N_2 adsorption/desorption isotherms show that the synthesized samples possess uniform mesoporosity. The average pore size of the samples is shown in Table 3 while Fig. 2 shows the pore size distribution using BJH model. The results show that all the samples exhibit hierarchical pore structure with mesoporosity range of 2–50 nm, and macroporosity range of 50–200 nm. The hierarchy factor of the samples is shown in Table 3. The XRD patterns show the characteristics of Y zeolite without the competing presence of any impurities. Further, the intensity of the characteristic peaks informs their crystallinity (Table 3). The formation of hierarchical nanoporous HY zeolite was also confirmed by FT-IR spectroscopy, as shown in Fig. 4. All the samples possess the characteristic peaks of Y zeolite at around 1002 and 460 cm^{-1}. The band 455–476 cm^{-1} are attributed to the O–T (Si or Al) bending vibrations [36], and the broad bands around 1000 cm^{-1} are attributed to the internal tetrahedral asymmetrical stretching vibration. Further, the bands at 558–572 cm^{-1} are ascribed to the hexatomic ring vibrations of Y zeolite [37,38], and the bands at 760–790 cm^{-1} are assigned to the external linkage symmetrical stretching vibrations.

SEM revealed the morphology of synthesized HY zeolites as illustrated in Fig. 5. All the samples show both the octahedral morphology attributed to conventional Y zeolite and globular particles with rugged surfaces, which confirms the mesoporosity of the samples [39].

Further, Table 4 presents the optimization results showing the sample responses.

3.1.1. Statistical analysis

The CCD arrangement of the three process variables in Table 1 enables development of mathematical model presenting each response as a function of aging time (X_1), crystallization time (X_2) and NaOH/solid ratio (X_3). Each response was computed as a function of the sum of a constant, three second-order effects, three first-order effects and three interaction effects of the process variables (Eq. (2)). Six replicated runs at the center point (runs 4, 5, 11, 12, 18 and 19) determined the residual error associated with the experiment. This error is an inexplicable variance in the experiment that significantly affects the reliability of the experiment as

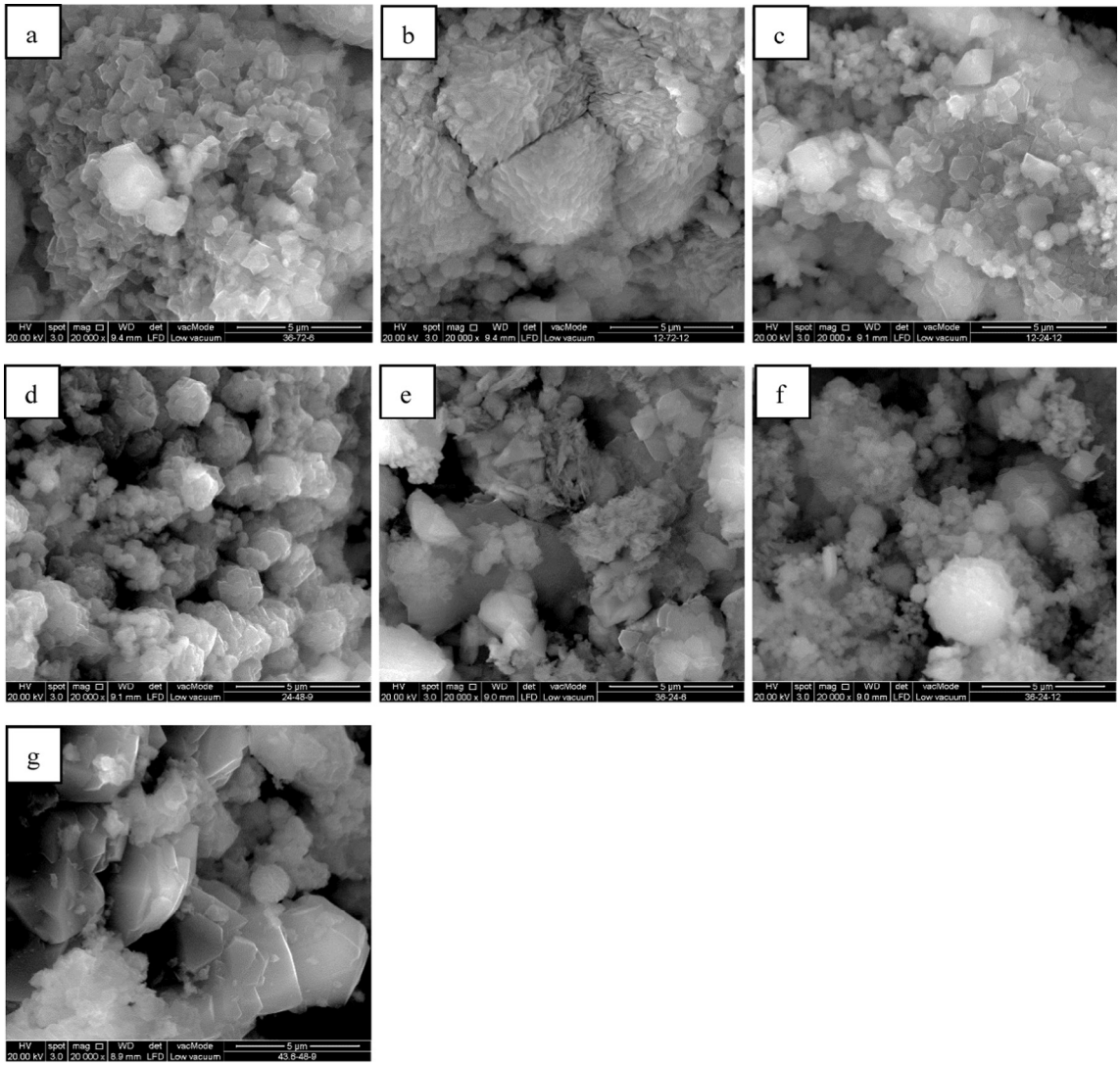

Fig. 5. SEM images of some selected HY zeolites samples. (a) HY36-72-6; (b) HY$_1$2-72-12; (c) HY12-24-12; (d) HY24-48-9; (e) HY36-24-6; (f) HY36-24-12; (g) HY43.6-48-9.

Table 4
Results of the response variables.

Run	Y_1	Y_2	Y_3
1	42.55	130.26	0.07
2	20.78	33.16	0.07
3	5.3143	22.79	0.02
4	74.07	349.45	0.24
5	75.09	350.21	0.24
6	85.64	406.14	0.23
7	16.09	80.46	0.13
8	73.61	325.08	0.21
9	106.86	443.78	0.30
10	40.57	165.72	0.17
11	78.15	366.62	0.22
12	74.94	353.34	0.22
13	83.19	319.98	0.29
14	31.32	133.24	0.11
15	84.41	363.82	0.21
16	63.79	394.84	0.18
17	74.93	366.90	0.20
18	76.62	359.06	0.23
19	77.98	361.46	0.22
20	87.29	367.34	0.32

well as the mathematical model. ANOVA helped to analyze the suitability of the proposed model.

The experimental data modeled into the second-order quadratic equation. Table 4 presents the results of the 3 response variables. Below are the full models for crystallinity (Y_1), SSA (Y_2) and HF (Y_3):

$$Y_1 = -70.028 - 2.028X_1 + 1.857X_2 + 32.818X_3 + 0.066X_1^2 - 0.016X_2^2 - 1.723X_3^2 + 0.001X_1X_2 - 0.099X_1X_3 - 0.08X_2X_3$$

$$Y_2 = -613.107 - 10.05X_1 + 12.471X_2 + 187.713X_3 + 0.307X_1^2 - 0.093X_2^2 - 9.16X_3^2 - 0.012X_1X_2 - 0.232X_1X_3 - 0.595X_2X_3$$

$$Y_3 = -0.278 - 0.0044X_1 + 0.0069X_2 + 0.0927X_3 + 0.0002X_1^2 - 0.0000X_2^2 - 0.0047X_3^2 + 0.000X_1X_2 - 0.0003X_1X_3 - 0.0003X_2X_3$$

Table 5 presents the model coefficients with their respective p-values. The significance of the terms in the model was measured by their p-values and F-values (Tables 5 and 6). A process variable has

Table 5
Proposed model for crystallinity, SSA and HF for hierarchical nanoporous HY zeolite formulation.

Term	Crystallinity		SSA		HF	
	Coeff	*p*-Value	Coeff	*p*-Value	Coeff	*p*-Value
β_0	−70.028	0.29	−613.107	0.075	−0.277947	0.251
Blocks	12.0976	0.004	60.408	0.004	0.035471	0.013
X_1	−2.0288	0.332	−10.05	0.327	−0.0044	0.556
X_2	1.8573	0.093	12.471	0.03	0.006919	0.087
X_3	32.8179	0.006	187.713	0.002	0.092658	0.02
X_1^2	0.0657	0.036	0.307	0.043	0.000165	0.123
X_2^2	−0.0163	0.036	−0.093	0.019	−0.000038	0.147
X_3^2	−1.7234	0.003	−9.16	0.002	−0.004646	0.015
X_1X_2	0.0009	0.96	−0.012	0.888	0.000005	0.941
X_1X_3	−0.0987	0.489	−0.232	0.737	−0.000271	0.6
X_2X_3	−0.0799	0.272	−0.595	0.109	−0.000338	0.207
R^2	0.8791		0.8773		0.8149	

Table 6
ANOVA for the predicted response models.

Source	DF	Seq SS	Adj SS	Adj MS	*F*-test	*F*-critical	*p*-Value
Crystallinity							
Blocks	1	2810	2809.96	2809.96	14.5		0.004
Model	9	9870.8	9870.81	1096.76	5.66	3.188	0.008
Linear	3	3764.6	3675.71	1225.24	6.32		0.014
Square	3	5739.7	5739.65	1913.22	9.87		0.003
Interaction	3	366.6	366.58	122.19	0.63		0.614
Residual error	9	1744.7	1744.67	193.85	0		
Lack-of-fit	5	1737.5	1737.49	347.5	193.54	6	0
Pure error	4	7.2	7.18	1.8			
Total	19	14425.5					
SSA							
Blocks	1	70,063	70,062	70062.1	15.08		0.004
Model	9	228,900	228,900	25433.4	5.48	3.188	0.009
Linear	3	56,057	122,438	40812.5	8.79		0.005
Square	3	157,522	157,522	52507.4	11.3		0.002
Interaction	3	15,321	15,321	5107.2	1.1		0.399
Residual error	9	41,808	41,808	41,808	4645.4		
Lack-of-fit	5	41,717	41,717	41,717	8343.4	6	0
Pure error	4	91	91	91	22.9		
Total	19	340,771					
HF							
Blocks	1	0.024158	0.024157	0.024157	9.41		0.013
Model	9	0.070404	0.070404	0.007823	3.05		0.056
Linear	3	0.026473	0.030668	0.010223	3.98		0.046
Square	3	0.03841	0.03841	0.012803	4.99		0.026
Interaction	3	0.00552	0.00552	0.00184	0.66		0.566
Residual error	9	0.023101	0.023101	0.002567	0		
Lack-of-fit	5	0.023001	0.023001	0.0046	183.42	6	0
Pure error	4	0.0001	0.0001	0.000025			
Total	19	0.117662					

Table 7
Margin of error for the response parameters at 95% confidence level.

Sample	Y_1	Y_2	Y_3
Standard deviation	27.55	133.92	0.079
Upper bound	12.69	61.68	0.036
Lower bound	−6.6	−32.08	−0.019

significance on a response only if the *p*-value is less than 0.05, or if the *F*-value is greater than its critical value. *F*-statistic can be written as

$$F = \frac{\mathrm{MSR}}{\mathrm{MSE}}$$

$$\mathrm{MSE} = \frac{\mathrm{SSE}}{\mathrm{DF}}$$

where MSR and MSE are the mean squares for models and residuals respectively, SSE is the sum of square for residuals and DF is the degree of freedom.

From Table 5, we can see that all the square terms significantly affects crystallinity and SSA; only X_3 is significant for crystallinity linearly while X_2 and X_3 affect SSA significantly, and X_3 and X_3^2 significantly affect the HF of the samples. It is clear that none of the interactions between the process variables affect any of the response.

3.2. Model significance check

The acceptability of the proposed models is investigated with ANOVA using 95% confidence level (Table 6). This analysis was performed using Minitab statistical software, which used mean square, based on the residual error (MSE) to compute *F*-value. The *F*-value for crystallinity, SSA, and HF models are 5.66, 5.48 and 3.05 respectively and the critical $F_{0.05,9,9}$ obtained from the table of critical value for *F* distribution is 3.18. Also, the *p*-value the model of crystallinity, SSA and HF are 0.008, 0.009 and 0.054 respectively. Therefore, it is clear that the *F*-values and *p*-values

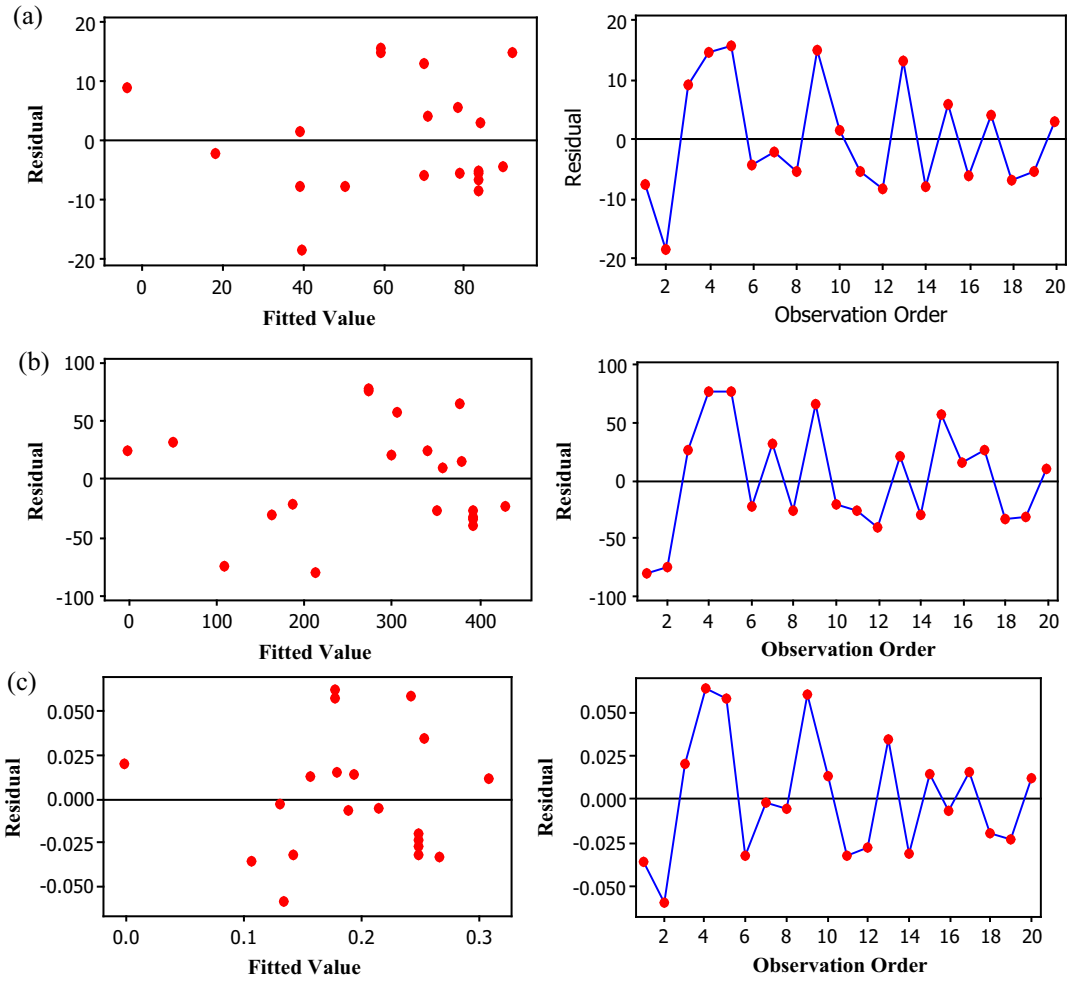

Fig. 6. Residual of fitted value (on the left) and observation order (on the right) for (a) crystallinity, (b) SSA, and (c) HF.

of the entire response model show that all the models are significant except that of HF. However, since the pure error is significantly lower than residual error, then the model shows significant lack-of-fit (0.00). Therefore, we use the mean square for pure error rather than MSE to re-compute *F*-value, then *F*-value of HF becomes 312.92 which is greater than the critical $F_{0.05,9,4}$ (6.00). This shows that HF model is also significant based on pure error due to significant lack-of-fit.

Table 7 shows the margin of error for the models. The lower bound is almost half of the upper bound. The observed discrepancies as shown in the table could be associated with uncertainty of position estimate [40,41].

To further, evaluate the effectiveness of the models with respect to sample quality, we compute the tolerance interval at 95% confidence level for each model as shown in Fig. 7. The top part of each section (a–c) presents the histograms of the response values, which shows the response distribution. It is clear that the distribution of all the responses are multimodal. The middle part of the sections show 2 different methods of determining tolerant interval; normal and nonparametric method. These give the tolerance interval of expected response from each model, that is, the normal interval and the nonparametric interval of the distribution. The normality test in the bottom part of each section in Fig. 6 shows that the sample data for all the responses are normally distributed. Therefore, the normal interval (−12.47 to 139.79% for Y_1; −85.35 to 654.71 cm^2/g for Y_2 and −0.024 to 0.411 for Y_3) is considered suitable. However, the lower limits are lower than the expected value range, which makes the range too wide. Consequently, the nonparametric (distribution-free) method becomes more appropriate. This gives interval 5.31–106.86% for Y_1; 22.79–443.78 cm^2/g for Y_2 and 0.019–0.319 for Y_3.

The plot of normal probability of the residuals for all the response variables revealed the normality of the recorded data. The plot gives an illustration that shows if the set of data obtained is approximately scattered or not. The residual plot shows the difference between the fitted and the experimental data of the regression model. Fig. 6 shows the studentized residuals versus the fitted values (estimated response) and observation order, which reveals that the residual data points are randomly scattered about zero, and suggests that there is no serial correlation between the residual error and the fitted values. This is an indication that no response transformation is required for this experimental design.

3.3. Effect of process variables

Figs 8–10 show the surface plots of sets of combination of two process variables, fixing the other variable for crystallinity, SSA and HF model. In the model for all the response variables, X_3 is the most significant process variable. This is because it exhibits the highest coefficient in the response models. However, X_3 shows no significant interaction with another process variable. Fig. 8 illustrates the dependence of crystallinity (Y_1) on the process variables. The plots exhibit curvature of three-dimensional faces. The crystallinity increases as the NaOH/solid ratio (X_3) decreases to its low level (6 ml/g). Y_1 also increase with crystallization time (X_2) towards the central level and latter decrease as X_2 increases. Con-

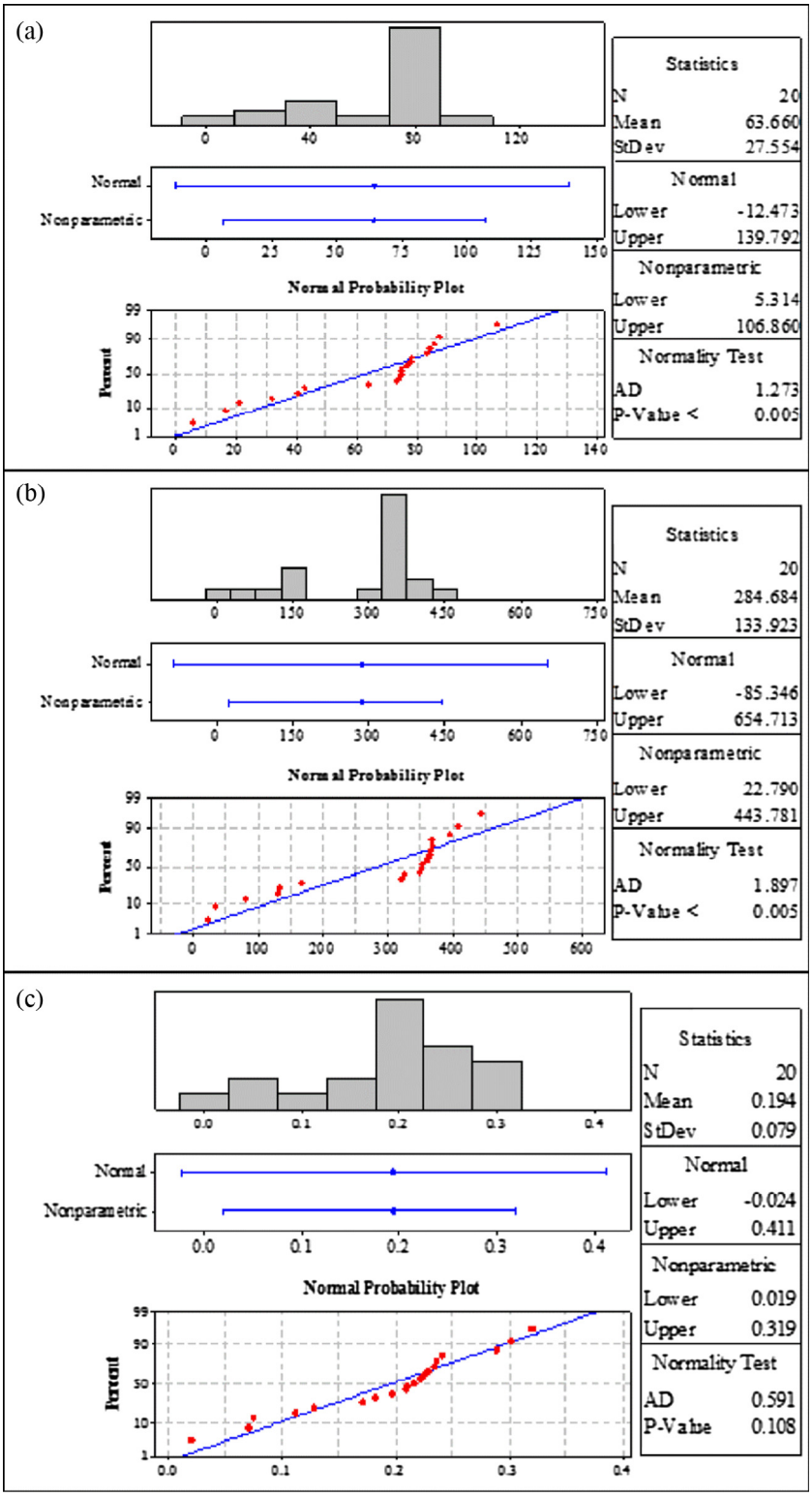

Fig. 7. Tolerance interval plot for (a) crystallinity, (b) SSA, and (c) HF.

versely, Y_1 sparingly decreases with increase in aging time (X_1) towards the center level and thereafter increases with X_1 to its high level. This indicates that the stronger effect of aging occurs at its high level meaning that aging is crucial to obtaining high purity Y zeolite. The surface plots of the effect of the process variables in Fig. 9 reveals that all the process variables significantly influenced SSA (Y_2). Initially, at the lowest X_1 (4.04 h) towards the center level, there is no significant change in the value of Y_2. As X_1 increased to the high level, Y_2 increases meaning that micropore volume increases with aging. At the lowest level of X_2, Y_2 is low but the increase in X_2 to the low level leads to a slight decrease in Y_2 towards high level and subsequent rapid decrease towards the highest level. Y_2 increased as X_3 increases to the lower level (6 ml/g) but further increase in X_3 leads to decrease in Y_2. Further,

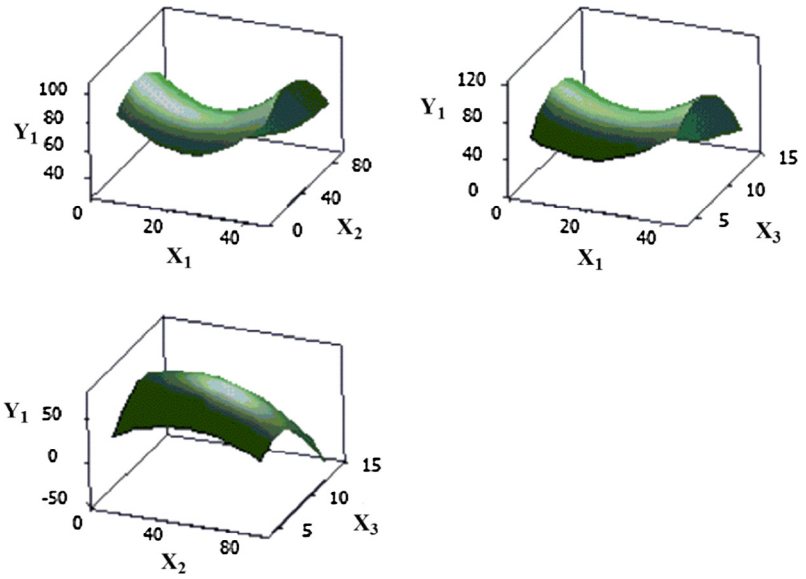

Fig. 8. Response surface plot showing the effect of process variables on crystallinity.

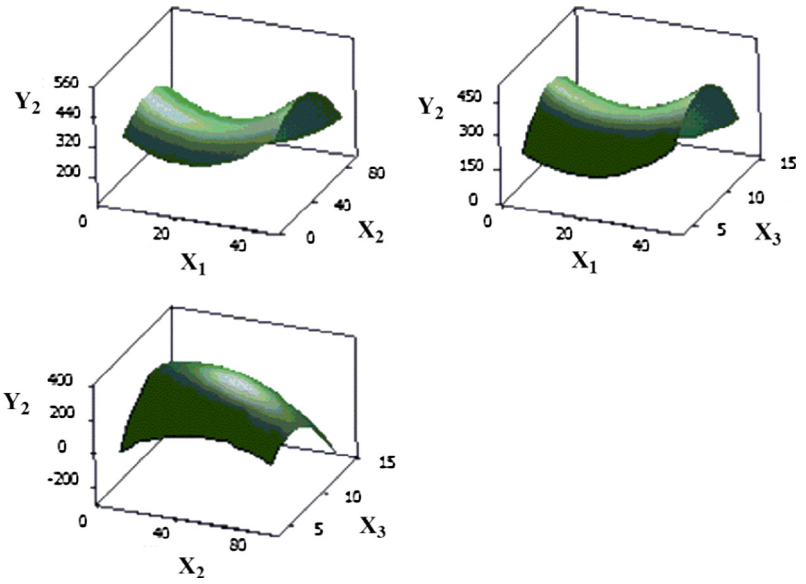

Fig. 9. Response surface plot showing the effect of process variables on specific surface area.

the effect of process variables in Fig. 10 indicates that all the factors affect the HF (Y_3). Y_3 increases with increase in X_1 and X_2, but the increase in X_2 towards its high level leads to decrease in Y_3. At the lowest level of X_3, Y_3 is low. However, increase in X_3 to the low-level increases Y_3. Meanwhile, a further increase in X_3 is detrimental to Y_3.

3.4. Optimization of process variables

Response optimizer helps in identification of a set of independent variable values that could jointly optimize the response variables. The suitability of the set of independent variables in satisfying the requirements of the targeted responses was measured by the term called composite desirability (D). Composite desirability is a tool for the assessment of how well a set of variables satisfies the defined goals for the responses. The value of D was obtained from the predetermined individual desirability (d) for each response. To maximize the composite desirability, multiple starting points reduced gradient algorithm was used. This helps to determine the optimal value of the process variables.

Fig. 11 presents the plots of all the responses and the sets of process variables and responses. It also includes the individual desirability of the process variables as well as the composite desirability. The optimum set of operating parameter for hierarchical nanoporous HY zeolites synthesis is; Aging time = 43. 60 h, crystallization time = 64.23 h and NaOH/solid ratio = 6.97 ml/g. The predicted responses are crystallinity = 99.95%, SSA = 442.73, HF = 0.33. This is in consonant with the report of Karami and Rohani [1] which states that the aging time varies from 40–120 h

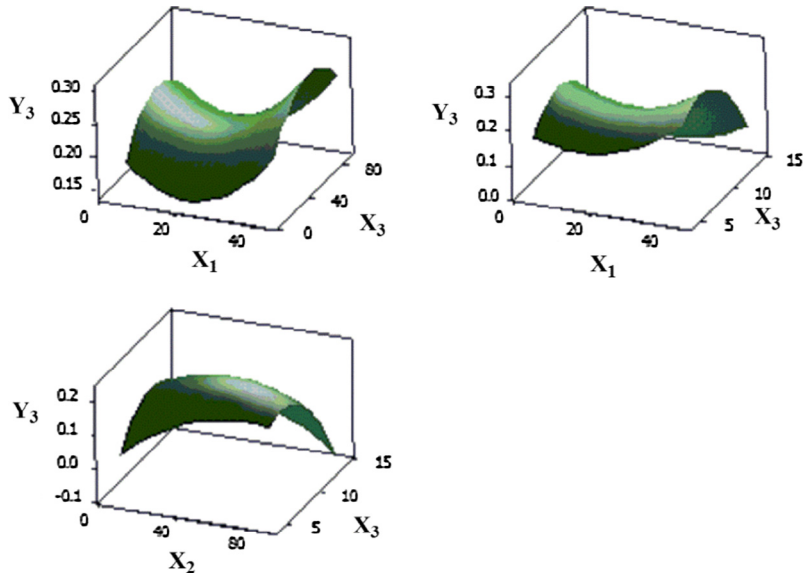

Fig. 10. Response surface plot showing the effect of process variables on hierarchy factor.

depending on the silica and alumina source. The value of composite desirability ranges from 0 to 1. For an ideal case, the value tends towards 1, while zero means one or more dependent variables are not within their acceptable limit. The value of the composite desirability obtained is 0.9021. This value is well acceptable because of its closeness to the ideal case. Furthermore, an experiment was performed by using the optimum values of the process variables, the error was estimated, and the result is presented in Table 8.

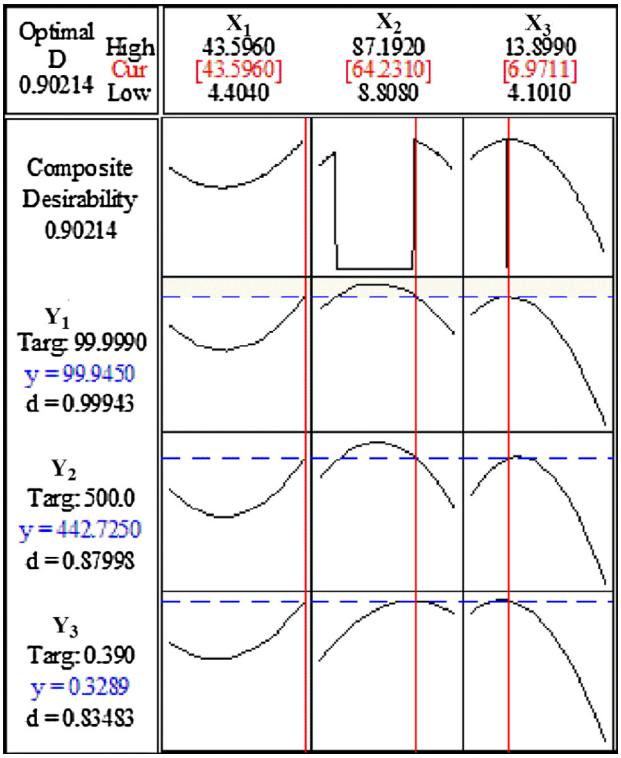

Fig. 11. Optimization plots for crystallinity, SSA and HF. (where D = composite desirability, d = individual desirability, Targ = target, cur = position of the cursor, y = value of response variables at optimal process variables, high and low means high and low levels of process variable in the DoE).

4. Conclusion

To describe the effect of aging time (X_1), crystallization time (X_2) and NaOH solution to kaolin ratio (X_3) on the properties of hierarchical nanoporous HY zeolite, RSM models based on CCD were developed. The responses under consideration are crystallinity (Y_1), SSA (Y_2) and HF (Y_3). X_3 was discovered to be the most significant process variable in the formulation of hierarchical nanoporous HY zeolite. Analysis of variance (ANOVA) and optimization study using response surface methodology (RSM) authenticated this observation. All the response models obtained for the HY zeolite synthesis showed p-value less than 0.05 and F-value higher than the critical value of F except HF. However, the F-value for HF was re-computed using mean square based on pure error rather than MSE. This gives F-value greater than its critical value. This reveals that the HF model is adequate but showed significant lack-of-fit. The optimum formulation for 99.95% crystallinity, 442.73 m^3/g BET surface area and 0.33 hierarchy factor (HF) was 43.60 h aging time, 64.23 h crystallization and 6.97 ml/g NaOH solution to kaolin ratio. Therefore, it is possible to develop an empirical model to predict the formulation for the synthesis of hierarchical nanoporous HY zeolite. Adjustment of all the process variables was found to be significant for C% and SSA while only X_3 has a significant effect on HF.

Acknowledgements

The authors gratefully acknowledge the financial support from GSP-MOHE (MO008-2015), University of Malaya, Malaysia.

Table 8
Comparison of the predicted and the experimental responses using the optimum value of process variables.

Aging time (X_1)	Crystallization time (X_2)	NaOH/solid (X_3)	Crystallinity (%) (Y_1)			BET SSA (cm^2/g) (Y_2)			HF (Y_3)		
(h)	(h)	(ml/g)	Pred.	Exp.	Error	Pred.	Exp.	Error	Pred.	Exp.	Error
43.60	64.23	6.97	99.95	94.35	5.6	443	428	15	0.33	0.31	0.02

References

[1] D. Karami, S. Rohani, Synthesis of pure zeolite Y using soluble silicate, a two-level factorial experimental design, Chem. Eng. Process. 48 (8) (2009) 1288–1292.

[2] P.A. Alaba, Y.M. Sani, W.M.A.W. Daud, Kaolinite properties and advances for solid acid and basic catalyst synthesis, RSC Adv. 5 (122) (2015) 101127–101147.

[3] P.A. Alaba et al., Synthesis and application of hierarchical mesoporous HZSM-5 for biodiesel production from shea butter, J. Taiwan Inst. Chem. Eng. 59 (2016) 405–412.

[4] I. Ivanova et al., Design of hierarchically structured catalysts by mordenites recrystallization: application in naphthalene alkylation, Catal. Today 168 (1) (2011) 133–139.

[5] P.A. Alaba, Y.M. Sani, W.M.A.W. Daud, Efficient biodiesel production via solid superacid catalysis: a critical review on recent breakthrough, RSC Adv. (2016).

[6] M.J. Verhoef et al., Partial transformation of MCM-41 material into zeolites: formation of nanosized MFI type crystallites, Chem. Mater. 13 (2) (2001) 683–687.

[7] I.Y. Mohammed et al., Catalytic intermediate pyrolysis of napier grass in a fixed bed reactor with ZSM-5, HZSM-5 and zinc-exchanged zeolite-A as the catalyst, Energies 9 (4) (2016) 246.

[8] C.J. Jacobsen et al., Mesoporous zeolite single crystals, J. Am. Chem. Soc. 122 (29) (2000) 7116–7117.

[9] P.A. Alaba, Y.M. Sani, W.M.A.W. Daud, A comparative study on thermal decomposition behavior of biodiesel samples produced from shea butter over micro-and mesoporous ZSM-5 zeolites using different kinetic models, J. Thermal Anal. Calorim. (2016) 1–6.

[10] Q. Tan et al., Synthesis, characterization, and catalytic properties of hydrothermally stable macro–meso–micro-porous composite materials synthesized via in situ assembly of preformed zeolite Y nanoclusters on kaolin, J. Catal. 251 (1) (2007) 69–79.

[11] Y. Han et al., Hydrothermally stable ordered hexagonal mesoporous aluminosilicates assembled from a triblock copolymer and preformed aluminosilicate precursors in strongly acidic media, Chem. Mater. 14 (3) (2002) 1144–1148.

[12] P.A. Alaba et al., Insight into catalyst deactivation mechanism and suppression techniques in thermocatalytic deoxygenation of bio-oil over zeolites, Rev. Chem. Eng. 32 (1) (2016) 71–91.

[13] Y.M. Sani et al., Acidity and catalytic performance of Yb-doped/Zr in comparison with/Zr catalysts synthesized via different preparatory conditions for biodiesel production, J. Taiwan Inst. Chem. Eng. 59 (2016) 195–204.

[14] Y.M. Sani et al., Facile synthesis of sulfated mesoporous Zr/ZSM-5 with improved Brønsted acidity and superior activity over SZr/Ag, SZr/Ti, and SZr/W in transforming UFO into biodiesel, J. Taiwan Inst. Chem. Eng. 60 (2016) 247–257.

[15] H.J. Köroğlu et al., Effects of low-temperature gel aging on the synthesis of zeolite Y at different alkalinities, J. Cryst. Growth 241 (4) (2002) 481–488.

[16] S. Yang, A.G. Vlessidis, N.P. Evmiridis, Influence of gel composition and crystallization conditions on the conventional synthesis of zeolites, Ind. Eng. Chem. Res. 36 (5) (1997) 1622–1631.

[17] M. Ahmadi et al., Application of the central composite design and response surface methodology to the advanced treatment of olive oil processing wastewater using Fenton's peroxidation, J. Hazard. Mater. 123 (1) (2005) 187–195.

[18] X. Liu et al., In situ synthesis of NaY zeolite with coal-based kaolin, J. Nat. Gas Chem. 12 (1) (2003) 63–70.

[19] S. Chandrasekhar, P. Pramada, Kaolin-based zeolite Y, a precursor for cordierite ceramics, Appl. Clay Sci. 27 (3) (2004) 187–198.

[20] P.A. Alaba, Y.M. Sani, W.M.A.W. Daud, Synthesis and characterization of hierarchical nanoporous HY zeolites from acid-activated kaolin, Chin. J. Catal. 36 (11) (2015) 1846–1851.

[21] P.A. Alaba et al., Synthesis and characterization of sulfated hierarchical nanoporous faujasite zeolite for efficient transesterification of shea butter, J. Clean. Prod. 142 (2017) 1987–1993, http://dx.doi.org/10.1016/j.jclepro.2016.11.085.

[22] N. Hosseinpour et al., Synergetic effects of Y-zeolite and amorphous silica-alumina as main FCC catalyst components on triisopropylbenzene cracking and coke formation, Fuel Process. Technol. 90 (2) (2009) 171–179.

[23] L. Frunz, R. Prins, G.D. Pirngruber, ZSM-5 precursors assembled to a mesoporous structure and its subsequent transformation into a zeolitic phase—from low to high catalytic activity, Microporous Mesoporous Mater. 88 (1) (2006) 152–162.

[24] J. Zheng et al., The hierarchical effects of zeolite composites in catalysis, Catal. Today 168 (1) (2011) 124–132.

[25] J. Zheng et al., Hierarchical porous zeolite composite with a core– shell structure fabricated using β-zeolite crystals as nutrients as well as cores, Chem. Mater. 22 (22) (2010) 6065–6074.

[26] J. Zheng et al., Synthesis of bi-phases composite zeolites MFZ and its hierarchical effects in isopropylbenzene catalytic cracking, Microporous Mesoporous Mater. 171 (2013) 44–52.

[27] T. Platz et al., Reliability and validity of arm function assessment with standardized guidelines for the Fugl-Meyer test, action research arm test and box and block test: a multicentre study, Clin. Rehabil. 19 (4) (2005) 404–411.

[28] P.A. Rosa, A.M. Azevedo, M.R. Aires-Barros, Application of central composite design to the optimisation of aqueous two-phase extraction of human antibodies, J. Chromatogr. A 1141 (1) (2007) 50–60.

[29] G.E. Box, W.G. Hunter, J.S. Hunter, Statistics for Experimenters: An Introduction to Design, Data Analysis, and Model Building, John Wiley & Sons Canada Ltd, Canada, 1978.

[30] D. Garrett, J. Pruitt, Problems encountered with the average potential method of analyzing substation grounding systems, IEEE Trans. Power Appar. Syst. 12 (1985) 3585–3596.

[31] S. Aud et al., The Condition of Education 2010. NCES 2010-028, National Center for Education Statistics, 2010.

[32] T.M. Meyer, M. Jenny, Measuring error for adjacent policy position estimates: dealing with uncertainty using CMP data, Elect. Stud. 32 (1) (2013) 174–185.

[33] Y.-H. Lai, Y.-F. Yen, L.-A. Chen, Validation of tolerance interval, J. Stat. Plan. Inference 142 (4) (2012) 902–907.

[34] M. Nourmohammadi, M.J. Jozani, B.C. Johnson, Distribution-free tolerance intervals with nomination samples: applications to mercury contamination in fish, Stat. Methodol. 26 (2015) 16–33.

[35] M.E. Zorn, R.D. Gibbons, W.C. Sonzogni, Evaluation of approximate methods for calculating the limit of detection and limit of quantification, Environ. Sci. Technol. 33 (13) (1999) 2291–2295.

[36] X. Zhang et al., Structural features of binary microporous zeolite composite Y-Beta and its hydrocracking performance, Catal. Today 149 (1) (2010) 212–217.

[37] B.A. Holmberg et al., Controlling size and yield of zeolite Y nanocrystals using tetramethylammonium bromide, Microporous Mesoporous Mater. 59 (1) (2003) 13–28.

[38] C. Kosanović et al., Study of the mechanism of formation of nano-crystalline zeolite X in heterogeneous system, Microporous Mesoporous Mater. 142 (1) (2011) 139–146.

[39] Z. Qin et al., A defect-based strategy for the preparation of mesoporous zeolite Y for high-performance catalytic cracking, J. Catal. 298 (2013) 102–111.

[40] A. Volkens, Quantifying the election programmes: coding procedures and controls. Mapping Policy Preferences: Parties, Electors and Governments: 1945–1998: Estimates for Parties, Electors and Governments 1945–1998, 2001, pp. 93–109.

[41] K. Benoit, M. Laver, S. Mikhaylov, Treating words as data with error: uncertainty in text statements of policy positions, Am. J. Polit. Sci. 53 (2) (2009) 495–513.